

Synthesis and Characterization of $\text{Li}_{1.035}\text{Mn}_{1.965}\text{O}_4$ and Al-doped $\text{Li}_{1.035}\text{Al}_{0.035}\text{Mn}_{1.930}\text{O}_4$ as Cathode Materials for Li-ion Batteries by a Wet-chemical Technique

KONG Long^{1,2}, LI Yun-Jiao^{1,2}, LI Wei-Jian², LI Pu-Liang², LI Hua-Cheng²

(1. School of Metallurgical Science and Engineering, Central South University, Changsha 410083, China; 2. Citic Dameng Mining Industries Limited, Nanning 530028, China)

Abstract: Spinel $\text{Li}_{1.035}\text{Mn}_{1.965}\text{O}_4$ and Al-doped $\text{Li}_{1.035}\text{Al}_{0.035}\text{Mn}_{1.930}\text{O}_4$ cathode materials were synthesized by a simple wet-chemical technique and heat treatment. The structure and the morphology of the two samples were investigated by powder X-ray diffraction (XRD), scanning electron microscope (SEM) and transmission electron microscope (TEM). The XRD patterns show that both of the two samples exhibit a well-defined spinel structure. The TEM result demonstrates that the $\text{Li}_{1.035}\text{Al}_{0.035}\text{Mn}_{1.930}\text{O}_4$ powder possesses a good crystalline state. The galvanostatic charge/discharge tests indicate that the $\text{Li}_{1.035}\text{Al}_{0.035}\text{Mn}_{1.930}\text{O}_4$ material delivers an excellent cycling ability and a nice rate capability, maintaining 96.4% of its initial capacity after 100 charge-discharge cycles at 0.5C and keeping 79.6% of the reversible capacity at 0.5C discharge rate when discharges at 4C rate.

Key words: LiMn_2O_4 ; Al substitution; wet-chemical technique; electrochemical performance

LiCoO_2 has been most widely used as a positive electrode material for lithium ion batteries since SONY company put it into commercial applications in 1991 because of its high capacity and easy synthesis^[1]. However, its poor rate performance, safety issues and the toxicity of cobalt hamper its large-scale commercial applications. The increasing demand for portable electronic devices and hybrid or full electric vehicles has motivated the study of other compounds, such as LiNiO_2 ^[2], LiFePO_4 ^[3], $\text{LiNi}_{1/3}\text{Co}_{1/3}\text{Mn}_{1/3}$ ^[4] and LiMn_2O_4 ^[5], etc. In particular, LiMn_2O_4 material shows several advantages, such as high potentials, low cost, low toxicity and good thermal stability^[6-7], which make it a promising cathode material. However, its capacity loss is the main issue to limit its large-scale use, especially at high temperature. This issue may attribute to several factors, including Jahn-Teller effect of trivalent manganese ions in the high spin state $t_{2g}^3e_g^1$ in the LiMn_2O_4 ^[8], and the dissolution of manganese ions into the electrolyte: $\text{Mn}^{3+} \rightarrow \text{Mn}^{2+} + \text{Mn}^{4+}$ ^[9]. To overcome this capacity fading problem, many efforts have been made to improve cycle life by seeking an appropriate synthesis method^[10-11] and doping a heterogeneous atom into the host LiMn_2O_4 structure^[12] or coating on the surface of LiMn_2O_4 ^[13].

In this work, three dimensional spinel lithium manganese oxides $\text{Li}_{1.035}\text{Mn}_{1.965}\text{O}_4$ and aluminum substituted $\text{Li}_{1.035}\text{Al}_{0.035}\text{Mn}_{1.930}\text{O}_4$ were synthesized by a wet-chemical technique combined with heat treatment using electrolytic manganese dioxide (EMD), lithium hydroxide (LiOH) and aluminum hydroxide as raw materials. The $\text{Li}_{1.035}\text{Al}_{0.035}\text{Mn}_{1.930}\text{O}_4$ sample shows the improved electrochemical properties of retention capacity and rate capability.

1 Experimental

1.1 Synthesis and characterization

$\text{Li}_{1.035}\text{Mn}_{1.965}\text{O}_4$ and Al-doped $\text{Li}_{1.035}\text{Mn}_{1.965}\text{O}_4$ cathodic materials were prepared by a simple wet-chemical process combined with heat treatment. EMD ($\text{Mn} \geq 59.36\%$, Xiangtan Chemical Industry), $\text{LiOH} \cdot \text{H}_2\text{O}$ (purity $\geq 98.9\%$, Sichuan Tianqi Lithium Industries, Inc., China) and $\text{Al}(\text{OH})_3$ (purity $\geq 98.9\%$, Tianjin Kermel, Inc., China) were used as raw materials. The precursors were prepared from the reaction of EMD with $\text{LiOH} \cdot \text{H}_2\text{O}$ and $\text{Al}(\text{OH})_3$ in aqueous solution at a required molar ratio of Li:Al:Mn. The precursors were preheated at 430°C for 12 h and then heated at 800°C for 12 h to obtain the final cathodic materials. A detailed description of the synthetic process has

Received date: 2012-07-18; Modified date: 2012-08-15; Published online: 2012-10-26

Foundation item: National Natural Science Foundation of China (50174058); Guangxi Zhuang Autonomous Region (Glorious Laurel Scholar Program, 2011)

Biography: KONG Long (1988-), male, Master degree candidate. E-mail: 670654388@qq.com

Corresponding author: LI Yun-Jiao, professor. E-mail: yunjiaoli6601@hotmail.com

been published in Reference [14].

The XRD patterns were recorded between 10° and 80° of 2θ at a scanning rate of $1^\circ/\text{s}$ using a Rigaku D/max-2500 X-ray powder diffractometer with $\text{Cu K}\alpha$ radiation. The particle morphologies of the products were carried out by SEM using JEOL JSM-6360LV operated at 20 kV. The TEM images were obtained on a Tecnai G12 microscope.

1.2 Electrochemical measurement

The working electrode was a mixture of 84wt% active material, 8wt% acetylene black and 8wt% PVDF binder and then the mixture was pressed into a film. A disk was cut off from the film and used as the cathode (13 mm diameter, *ca.* 200 μm). A typical weight of the cathode was 4–5 mg. The electrolyte was based on 1 mol/L LiPF_6 in a 1:1 (volume ratio) mixture of ethylene carbonate (EC) and dimethyl carbonate (DMC) and a thin polypropylene film was used as the separator. The 2016 cells were assembled in an argon-filled glove box and were charged and discharged at different rates ($1\text{C}=\text{mAh/g}$) with cut-off voltage 4.3 and 3.0 V at room temperature using Land (CT2001A) cell systems.

2 Results and discussion

2.1 Morphology and structure of the materials

The XRD patterns of the as-prepared $\text{Li}_{1.035}\text{Mn}_{1.965}\text{O}_4$ and $\text{Li}_{1.035}\text{Al}_{0.035}\text{Mn}_{1.930}\text{O}_4$ samples are shown in Fig. 1. Both of the two samples are identified as a single-phase spinel (JCPDS 35-0782) with a space group $\text{Fd}\bar{3}\text{m}$ where Li^+ ions locate on the 8a sites, Mn^{3+} , Mn^{4+} and Al^{3+} ions reside at the octahedral 16(d) sites and O^{2-} ions occupy the 32(e) sites^[15]. The shifting peak to larger 2θ angle can be attributed to the difference in ionic radius between Al^{3+} (0.053 nm) and Mn^{3+} (0.065 nm)^[16]. The lattice constant obtained from the Rietvelt refinement on the XRD data decreases by doping Al in the host structure of $\text{Li}_{1.035}\text{Mn}_{1.965}\text{O}_4$. For example, the undoped sample delivers the spinel lattice constant of 0.8237 nm, while the Al-doped sample lattice constant decreases to 0.8231 nm. The small substitution of Al^{3+} for Mn^{3+} reduces the lattice parameters and increases the bonding covalency of Mn–O as well as the strength of the framework of the intercalation compound.

Typical powder morphologies of the $\text{Li}_{1.035}\text{Mn}_{1.965}\text{O}_4$ and Al-doped $\text{Li}_{1.035}\text{Al}_{0.035}\text{Mn}_{1.930}\text{O}_4$ powders are shown in Fig. 2. Both samples have an average size of about 300 nm and show uniform particles.

To further understand the morphology and microstructure details of the $\text{Li}_{1.035}\text{Al}_{0.035}\text{Mn}_{1.930}\text{O}_4$ powders, the TEM image, selected area electron diffraction (SAED) pattern and high-resolution transmission electron micros-

copy (HRTEM), are performed. From the TEM image (Fig. 3(a)), interference fringes are observed on fine particles. The SAED pattern taken from $\text{Li}_{1.035}\text{Al}_{0.035}\text{Mn}_{1.930}\text{O}_4$ powder is shown in Fig. 3(b). The diffraction spots, from inner to outer, correspond to the (111), (311), (400), (440) diffraction planes of spinel LiMn_2O_4 , respectively, which indicate that Al ions are distributed homogeneously in the spinel structure without impurity phases existing in the doped sample. A layer separation of 0.245 nm, which corresponds to (400) plane in bulk LiMn_2O_4 , is observed in the HRTEM image (Fig. 3(c)).

2.2 Electrochemical performance

Figure 4(a) presents the discharge profiles of the pristine and Al-doped samples at 0.1C rate. Both of these two samples deliver two typical characteristic plateaus at 4 V. It is reported that the first voltage plateau is induced by $\lambda\text{-MnO}_2$ inlaid into Li^+ to form $\text{Li}_{0.5}\text{Mn}_2\text{O}_4$ and the second voltage plateau is induced by $\text{Li}_{0.5}\text{Mn}_2\text{O}_4$ inlaid into Li^+ to form LiMn_2O_4 ^[17]. The initial capacity of the Al-doped sample (116.2 mAh/g) is lower than the undoped one (117.5 mAh/g), which is due to the substitution of Al^{3+} for Mn^{3+} . But the small Al substitution results in the sample exhibiting a better rate performance. Figure 4(b) shows that at 4C rate, Al-doped sample gives a discharge capacity of over 90.6 mAh/g, which is higher than that of the pristine sample (74.3 mAh/g). Figure 4(c) shows the cy-

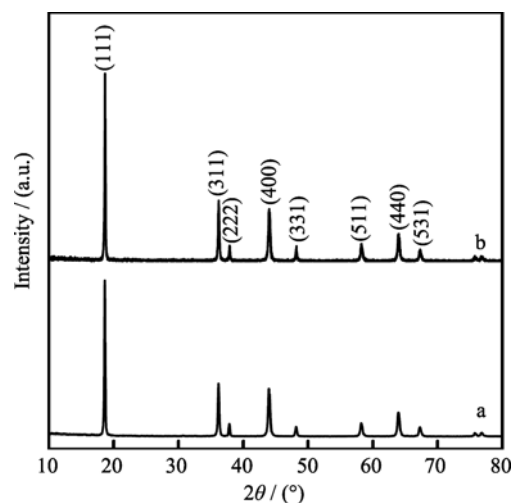


Fig. 1 XRD patterns of (a) $\text{Li}_{1.035}\text{Mn}_{1.965}\text{O}_4$ and (b) $\text{Li}_{1.035}\text{Al}_{0.035}\text{Mn}_{1.930}\text{O}_4$ powders

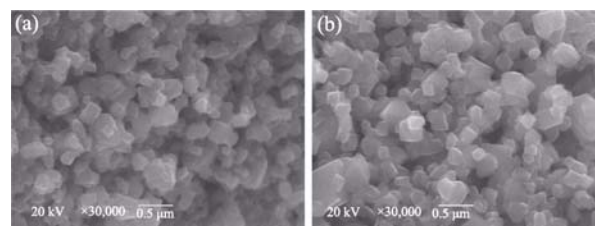


Fig. 2 SEM images of (a) $\text{Li}_{1.035}\text{Mn}_{1.965}\text{O}_4$ and (b) Al-doped $\text{Li}_{1.035}\text{Al}_{0.035}\text{Mn}_{1.930}\text{O}_4$ powders

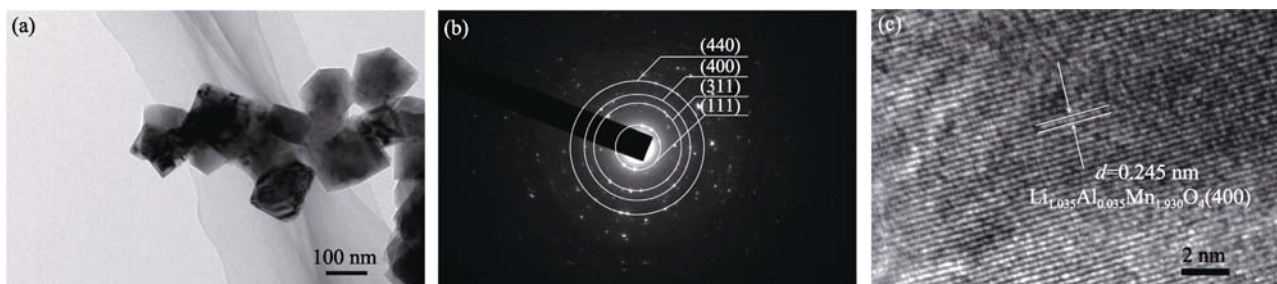


Fig. 3 Images and of the as-prepared $\text{Li}_{1.035}\text{Al}_{0.035}\text{Mn}_{1.930}\text{O}_4$ powder (a)TEM, SAED (b) and HRTEM (c)

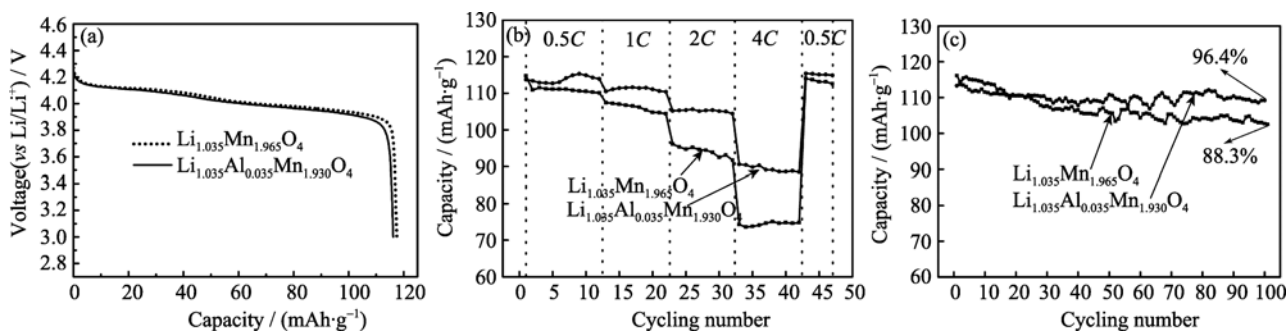


Fig. 4 (a) Discharge profiles at 0.1C rate, (b) discharge capacity with cycling number at different current rates and (c) cycling performances at 0.5C rate of $\text{Li}_{1.035}\text{Mn}_{1.965}\text{O}_4$ and Al-doped $\text{Li}_{1.035}\text{Al}_{0.035}\text{Mn}_{1.930}\text{O}_4$ powders

cling performances of the $\text{Li}_{1.035}\text{Mn}_{1.965}\text{O}_4$ and the $\text{Li}_{1.035}\text{Al}_{0.035}\text{Mn}_{1.930}\text{O}_4$ powders at 0.5C rate. The $\text{Li}_{1.035}\text{Al}_{0.035}\text{Mn}_{1.930}\text{O}_4$ sample displays a capacity retention ratio of 96.4% after 100 cycles, which is higher than that of the undoped sample (88.3%). The improvement of the cycling performance can be accounted for the high structural stability during the electrochemical cycling, because of the stronger Al–O bond (512 kJ/mol) compared to the Mn–O bond (402 kJ/mol) in the octahedron^[18]. What's more, the reduction of Mn^{3+} ions by doping Al can suppress the Jahn-Teller effect and cause less Mn dissolution, which leads to a higher capacity and a better cycling performance.

To investigate changes of the electrode/electrolyte interface, which may contribute to the different electrochemical performances between the $\text{Li}_{1.035}\text{Mn}_{1.965}\text{O}_4$ and $\text{Li}_{1.035}\text{Al}_{0.035}\text{Mn}_{1.930}\text{O}_4$ electrodes, the electrochemical impedance spectra (EIS) are carried out in the discharged state after three cycles. The Nyquist plots are presented in Fig. 5. It can be seen that each spectrum contains one semicircle in the high frequency region and a straight sloping line in the low frequency region. The high-frequency semicircle is from the charge-transfer process, and the straight line is attributed to the diffusion of lithium ions in the spinel^[19]. The EIS is fitted by the ZView 2.70 software. The corresponding equivalent circuit is inserted in Fig. 5. Here R_s is the resistance of the ohmic electrolyte, R_{ct} is the charge transfer resistance at the particle/electrolyte interface, and CPE1 represents the double layer capacitance and Z_w the Warburg impedance.

Table 1 lists the results calculated from ac impedance spectra based on the equivalent circuit shown in Fig. 5. It can be seen that both R_s and R_{ct} of the Al-doped sample are smaller than those of the undoped one. For example, the value of the charge transfer resistance R_{ct} for $\text{Li}_{1.035}\text{Al}_{0.035}\text{Mn}_{1.930}\text{O}_4$ sample is 83.49 Ω/cm^2 , which is much lower than the undoped sample (129.4 Ω/cm^2). This indicates that the small Al ions doping can effectively en-

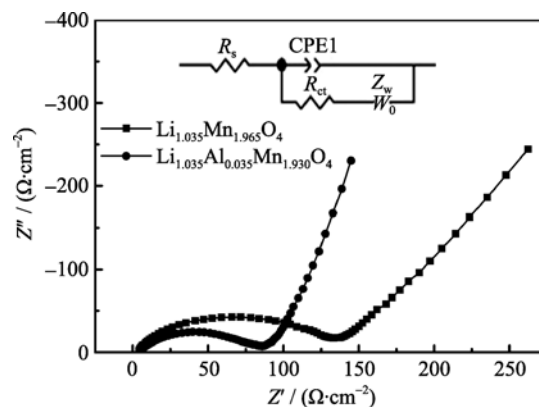


Fig. 5 Electrochemical impedance spectra (EIS) of the two samples in the discharged state (about 3.0 V, vs Li^+/Li) after 3 cycles with an equivalent circuit diagram is inserted

Table 1 The impedance parameters of $\text{Li}_{1.035}\text{Mn}_{1.965}\text{O}_4$ and $\text{Li}_{1.035}\text{Al}_{0.035}\text{Mn}_{1.930}\text{O}_4$ samples

Samples	R_s/Ω	R_{ct}/Ω
$\text{Li}_{1.035}\text{Mn}_{1.965}\text{O}_4$	4.32	129.4
$\text{Li}_{1.035}\text{Al}_{0.035}\text{Mn}_{1.930}\text{O}_4$	3.79	83.49

hance the electrical conductivity and decrease electrochemical polarization which contributes to improved rate capability.

3 Conclusions

Spinel $\text{Li}_{1.035}\text{Al}_x\text{Mn}_{1.965-x}\text{O}_4$ powders are prepared by a wet-chemical process followed by heat treatment. The XRD results reveal that the Al-doped sample is well crystallized to a single spinel structure with Fd3m space group. The TEM result demonstrates that the $\text{Li}_{1.035}\text{Al}_{0.035}\text{Mn}_{1.930}\text{O}_4$ powder possesses a good crystalline state. Electrochemical experiments show that the $\text{Li}_{1.035}\text{Al}_{0.035}\text{Mn}_{1.930}\text{O}_4$ material exhibits a high capacity, an excellent cycling ability and a nice rate capability, maintaining 96.4% of its initial capacity after 100 charge-discharge cycles at 0.5C rate, and keeping more than 79.6% of the reversible capacity at 0.5C discharge rate when discharged at 4C rate. EIS shows that both R_s and R_{ct} of the Al-doped samples are smaller than those of the undoped one. These results reveal that the small Al substitution of $\text{Li}_{1.035}\text{Mn}_{1.965}\text{O}_4$ in the wet-chemical synthesis is an effective method for improving the performance of spinel LiMn_2O_4 for lithium rechargeable batteries.

References:

- [1] Nishi Y. Lithium ion secondary batteries; past 10 years and the future. *Journal of Power Sources*, 2001, **100(1/2)**: 101–106.
- [2] Yamada S, Fujiwara M, Kanda M. Synthesis and properties of LiNiO_2 as cathode material for secondary batteries. *Journal of Power Sources*, 1995, **54(2)**: 209–213.
- [3] Gu L, Zhu C, Li H, *et al.* Direct observation of lithium staging in partially delithiated LiFePO_4 at atomic resolution. *Journal of the American Chemical Society*, 2011, **133(13)**: 4661–4663.
- [4] Lin Y K, Lu C H. Preparation and electrochemical properties of layer-structured $\text{LiNi}_{1/3}\text{Co}_{1/3}\text{Mn}_{1/3-y}\text{Al}_y\text{O}_2$. *Journal of Power Sources*, 2009, **189(1)**: 353–358.
- [5] Kim D K, Muralidharan P, Lee H W, *et al.* Spinel LiMn_2O_4 nanorods as lithium ion battery cathodes. *Nano Letters*, 2008, **8(11)**: 3948–3952.
- [6] Tarascon J M, Armand M. Issues and challenges facing rechargeable lithium batteries. *Nature*, 2001, **414**: 359–367.
- [7] Bhat M, Chakravarthy B, Ramakrishnan P, *et al.* Microwave synthesis of electrode materials for lithium batteries. *Bulletin of Materials Science*, 2000, **23(6)**: 461–466.
- [8] Yamada A, Tanaka M. Jahn-Teller structural phase transition around 280 K in LiMn_2O_4 . *Materials Research Bulletin*, 1995, **30(6)**: 715–721.
- [9] Lee S W, Kim K S, Lee K L, *et al.* Electrochemical characteristics of metal oxide-coated lithium manganese oxide (spinel type): Part II. In the range of 3.0–4.4 V. *Journal of Power Sources*, 2004, **130**: 233–240.
- [10] Lee H W, Muralidharan P, Ruffo R, *et al.* Ultrathin spinel LiMn_2O_4 nanowires as high power cathode materials for Li-ion batteries. *Nano Letters*, 2010, **10(10)**: 3852–3856.
- [11] Fu Y P, Su Y H, Lin C H, *et al.* Comparison of the microwave-induced combustion and solid-state reaction for the synthesis of LiMn_2O_4 powder and their electrochemical properties. *Ceramics International*, 2009, **35(8)**: 3463–3468.
- [12] Arillo M A, Cuello G, López M L, *et al.* Structural characterisation and physical properties of LiMMnO_4 (M=Cr, Ti) spinels. *Solid State Sciences*, 2005, **7(1)**: 25–32.
- [13] Li C, Zhang H P, Fu L J, *et al.* Cathode materials modified by surface coating for lithium ion batteries. *Electrochimica Acta*, 2006, **51(19)**: 3872–3883.
- [14] Li Y J, Kong L, Xi X M, *et al.* Hydrothermal Preparation and Characterization of LiMn_2O_4 for Li-ion Battery Application. Proceedings of COM 2012. Niagara Falls, Ontario, Canada, 2012.
- [15] Zhou W J, Bao S J, He B L, *et al.* Synthesis and electrochemical properties of $\text{LiAl}_{0.05}\text{Mn}_{1.95}\text{O}_4$ by the ultrasonic assisted rheological phase method. *Electrochimica Acta*, 2006, **51(22)**: 4701–4708.
- [16] Liang Y Y, Bao S J, Li H L. A series of spinel phase cathode materials prepared by a simple hydrothermal process for rechargeable lithium batteries. *Journal of Solid State Chemistry*, 2006, **179(7)**: 2133–2140.
- [17] Hung F Y, Lui T S, Liao H C. A study of nano-sized surface coating on LiMn_2O_4 materials. *Applied Surface Science*, 2007, **253(18)**: 7443–7448.
- [18] Sun Y K, Yoon C S, Kim C K, *et al.* Degradation mechanism of spinel $\text{LiAl}_{0.2}\text{Mn}_{1.8}\text{O}_4$ cathode materials on high temperature cycling. *Journal of Materials Chemistry*, 2001, **11(10)**: 2519–2522.
- [19] Hjelm A K, Lindbergh G. Experimental and theoretical analysis of LiMn_2O_4 cathodes for use in rechargeable lithium batteries by electrochemical impedance spectroscopy (EIS). *Electrochimica Acta*, 2002, **47(11)**: 1747–1759.

湿化学法合成富锂和掺铝尖晶石型锰酸锂及其电性能的改善

孔龙^{1,2}, 李运姣^{1,2}, 李维健², 李普良², 李华成²

(1. 中南大学 冶金科学与工程学院, 长沙 410083; 2. 中信大锰矿业有限责任公司, 南宁 530028)

摘要: 采用湿化学法-后续热处理技术, 合成了尖晶石型锰酸锂正极材料 $\text{Li}_{1.035}\text{Mn}_{1.965}\text{O}_4$ 和 $\text{Li}_{1.035}\text{Al}_{0.035}\text{Mn}_{1.930}\text{O}_4$ 。X射线衍射(XRD)结果表明这两种材料呈现出良好的尖晶石型结构。透射电子显微镜(TEM)表明 $\text{Li}_{1.035}\text{Al}_{0.035}\text{Mn}_{1.930}\text{O}_4$ 材料具有很好的结晶态。充放电测试表明 $\text{Li}_{1.035}\text{Al}_{0.035}\text{Mn}_{1.930}\text{O}_4$ 材料具有优良的循环性能和倍率性能: 以 0.5C 充放电, 经过 100 次循环后放电容量保持率为 96.4%, 经过 4C 放电后仍然能够保持 0.5C 放电态容量的 79.6%。

关键词: LiMn_2O_4 ; Al 掺杂; 湿化学法; 电化学性能

中图分类号: TM912

文献标识码: A